Since January 2020 Elsevier has created a COVID-19 resource centre with free information in English and Mandarin on the novel coronavirus COVID-19. The COVID-19 resource centre is hosted on Elsevier Connect, the company's public news and information website.

Article

Cell Reports

The Intergenic Recombinant HLA-B*46:01 Has a Distinctive Peptidome that Includes KIR2DL3 Ligands

Graphical Abstract

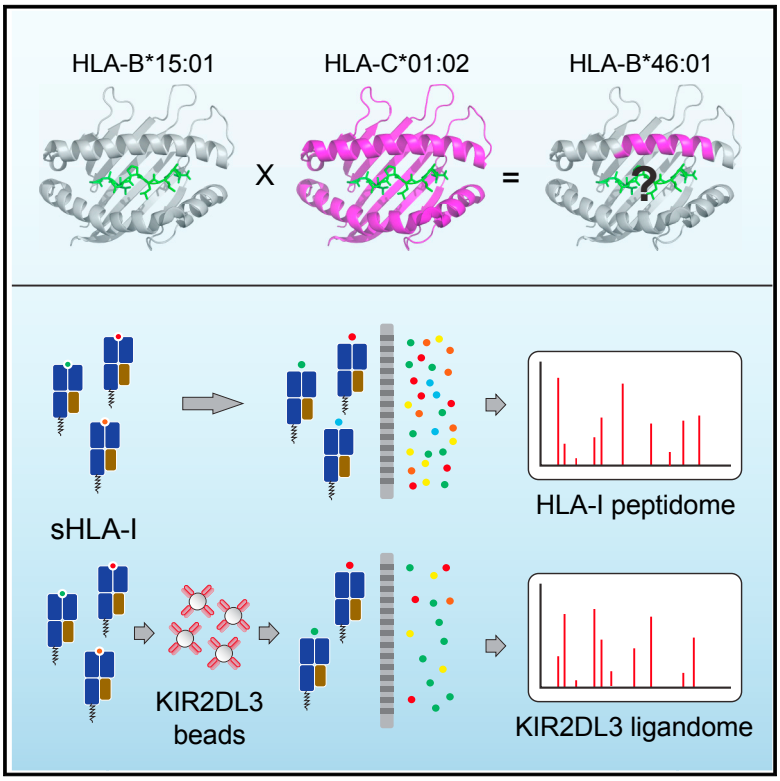

Highlights

- The interlocus recombinant *HLA-B*46:01* is found at high frequency in Southeast Asia
- HLA-B*46:01 has a low-diversity peptidome that is distinct from both its parents
- A subset of HLA-B*46:01 peptides provides ligands for the NK cell receptor KIR2DL3
- The unique features of HLA-B*46:01 correlate with protection against leprosy

Authors

Hugo G. Hilton, Curtis P. McMurtrey, Alex S. Han, ..., K. Christopher Garcia, William H. Hildebrand, Peter Parham

Correspondence

hghhilton@gmail.com

In Brief

Hilton et al. show how the recombination that formed *HLA-B*46:01* endowed it with a distinctive peptidome and unique functional properties. These properties likely protect carriers from severe infection with *Mycobacterium leprae*, the cause of leprosy, and they may account for the high frequency of *HLA-B*46:01* in Southeast Asia.

Hilton et al., 2017, Cell Reports *19*, 1394–1405
May 16, 2017
http://dx.doi.org/10.1016/j.celrep.2017.04.059

OPEN ACCESS
CellPress

Cell Reports
Article

The Intergenic Recombinant HLA-B*46:01 Has a Distinctive Peptidome that Includes KIR2DL3 Ligands

Hugo G. Hilton,[1,2,8,*] Curtis P. McMurtrey,[3] Alex S. Han,[1,2] Zakia Djaoud,[1,2] Lisbeth A. Guethlein,[1,2] Jeroen H. Blokhuis,[1,2] Jason L. Pugh,[1,2] Ana Goyos,[1,2] Amir Horowitz,[1,2] Rico Buchli,[4] Ken W. Jackson,[3] Wilfred Bardet,[3] David A. Bushnell,[1] Philip J. Robinson,[1] Juan L. Mendoza,[1,5] Michael E. Birnbaum,[1,5] Morten Nielsen,[6,7] K. Christopher Garcia,[1,5] William H. Hildebrand,[3] and Peter Parham[1,2]

[1]Department of Structural Biology, School of Medicine, Stanford University, Stanford, CA 94305, USA
[2]Department of Microbiology & Immunology, School of Medicine, Stanford University, Stanford, CA 94305, USA
[3]Department of Microbiology & Immunology, University of Oklahoma Health Sciences Center, Oklahoma City, OK 73104, USA
[4]Pure Protein LLC, Oklahoma City, OK 73104, USA
[5]Department of Molecular & Cellular Physiology, School of Medicine, Stanford University, Stanford, CA 94305, USA
[6]Department of Bio and Health Informatics, Technical University of Denmark, 2800 Kgs. Lyngby, Denmark
[7]Instituto de Investigaciones Biotecnológicas, Universidad Nacional de San Martín, Buenos Aires, Argentina
[8]Lead Contact
*Correspondence: hghhilton@gmail.com
http://dx.doi.org/10.1016/j.celrep.2017.04.059

SUMMARY

HLA-B*46:01 **was formed by an intergenic mini-conversion, between *HLA-B*15:01* and *HLA-C*01:02*, in Southeast Asia during the last 50,000 years, and it has since become the most common *HLA-B* allele in the region. A functional effect of the mini-conversion was introduction of the C1 epitope into HLA-B*46:01, making it an exceptional HLA-B allotype that is recognized by the C1-specific natural killer (NK) cell receptor KIR2DL3. High-resolution mass spectrometry showed that HLA-B*46:01 has a low-diversity peptidome that is distinct from those of its parents. A minority (21%) of HLA-B*46:01 peptides, with common C-terminal characteristics, form ligands for KIR2DL3. The HLA-B*46:01 peptidome is predicted to be enriched for peptide antigens derived from *Mycobacterium leprae*. Overall, the results indicate that the distinctive peptidome and functions of HLA-B*46:01 provide carriers with resistance to leprosy, which drove its rapid rise in frequency in Southeast Asia.**

INTRODUCTION

Population expansion, cultural changes, and migration during the last 100,000 years exposed humans to pathogens against which they had not evolved effective resistance. Host genetics strongly influence susceptibility to infectious disease, with pathogens that affect reproductive fitness imposing selection on genes that impact disease outcomes (Karlsson et al., 2014). Nowhere in the human genome are these effects more evident than in the *HLA* region (Parham, 2005). Because of their vital role in providing immunity against diverse and rapidly evolving pathogens, the *HLA-A*, *-B*, and *-C* genes have been subject to strong balancing selection, making them the most diverse of human genes (Barreiro and Quintana-Murci, 2010; Trowsdale, 2011). *HLA-A*, *-B*, and *-C* arose by a series of gene duplications from a common ancestral *MHC class I* gene (Parham et al., 1995). These genes also serve as a reservoir of polymorphic sequences that can be recombined to create new *HLA* alleles that can provide protection against emerging pathogens. Although such new variants are thought to arise in human populations during episodes of Darwinian selection, there is little direct evidence for the nature of the process. *HLA-B*46:01* provides a compelling example of such an episode.

*HLA-B*46:01* has restricted distribution in Southeast Asia where it likely originated around the time of the arrival of modern humans ~50,000 years ago (Abi-Rached et al., 2010; González-Galarza et al., 2015). It most likely rose in frequency following a selective sweep of the type more often seen in small, isolated populations (Abi-Rached et al., 2010), and it is now carried by ~110 million individuals of Southeast Asian descent (González-Galarza et al., 2015). Despite its high frequency, *HLA-B*46:01* is an unusual allele, formed by the recombination between *HLA-B*15:01* and *HLA-C*01:02*. Similar intergenic recombinants have been identified (Hildebrand et al., 1992; Steiner et al., 2002), but none is found at comparable frequency, suggesting that *HLA-B*46:01* fills an immunological niche not afforded by either parent or any other *HLA class I* variant found in the region. Supporting this notion, epidemiologic studies suggest that *HLA-B*46:01* may confer protection against *Mycobacterium leprae*, the causative agent of leprosy, which is endemic to Southeast Asia (Wang et al., 1999).

HLA class I glycoproteins are found on virtually all human cells, where they act as ligands for the killer-cell immunoglobulin-like receptors (KIRs) of natural killer (NK) cells and the T cell receptors (TCRs) of cytotoxic CD8 T cells (Colonna and Samaridis,

1995; Zinkernagel and Doherty, 1974). A key feature of HLA class I is a short peptide, produced by intracellular protein degradation, that is bound during assembly of the HLA in the endoplasmic reticulum. KIRs and TCRs recognize the upper face of HLA and its bound peptide (Boyington et al., 2000; Fan et al., 2001; Garboczi et al., 1996). TCR recognition is exquisitely sensitive to the sequence of the bound peptide. KIR binding appears less so, though the rules that govern the peptide specificity of KIR have yet to be fully defined.

Structural, functional, and genetic studies of *HLA class I* and its counterparts in non-human primates support a model in which *HLA-A* and *-B* evolved to become the major TCR ligands, whereas *HLA-C* evolved the C1 and C2 epitopes to become the principal KIR ligands (Guethlein et al., 2015). In this context, HLA-B*46:01 is an exceptional allotype that carries the C1 epitope and functions as a KIR ligand (Barber et al., 1996; Zemmour et al., 1992). As part of their functional specialization, HLA-A, -B, and -C bind distinctive sets of peptides and are distinguished by locus-specific polymorphisms and differences in cell-surface expression (McCutcheon et al., 1995; Sibilio et al., 2008; Turner et al., 1998; Zemmour and Parham, 1992).

HLA-B*46:01 differs from HLA-B*15:01 at residues 66–76 of the α_1 helix that derive from HLA-C*01:02 (Zemmour et al., 1992). Within this 11-residue segment, HLA-B*46:01 differs from HLA-B*15:01 at seven positions (K66I, Y67S, R69T, Q70N, A71T, D74Y, and V76E). Val76 is essential for the C1 epitope (Barber et al., 1996; Biassoni et al., 1995), and the KYRV motif at positions 66, 67, 69, and 76 reduces cell-surface expression of HLA-B*46:01 (Sibilio et al., 2008). Contributing to the TCR- and KIR-binding sites are residues 66, 69, 70, 71, 74, and 76 (Boyington et al., 2000; Fan et al., 2001; Garboczi et al., 1996). Because residues 66–76 comprise half of the polymorphic positions in the binding groove, they are predicted to influence the peptide-binding specificity of HLA-B*46:01.

Prior to this study, knowledge of the HLA-B*46:01 peptidome was limited to six peptides (Barber et al., 1996). Here we define at high resolution the peptidomes of HLA-B*46:01 and its parents. We then identify those peptides that provide ligands for the C1-specific NK cell receptor, KIR2DL3. Comparison of >6,000 HLA-B*15:01-binding peptides, >2,000 HLA-B*46:01-binding peptides, and >750 HLA-C*01:02-binding peptides shows how the recombination that created HLA-B*46:01 gave it a peptidome that is completely different from that of its parents. Its distinctive peptide-binding site appears well suited to bind antigenic peptides derived from *M. leprae*.

RESULTS

HLA-B*46:01, HLA-B*15:01, and HLA-C*01:02 Have Distinctive Peptidomes

To compare the peptides bound by HLA-B*46:01 and its parental allotypes, we isolated these HLA molecules, eluted the bound peptides, and determined their sequences by mass spectrometry. We identified 6,387 peptides for HLA-B*15:01, 788 for HLA-C*01:02, and 2,115 for HLA-B*46:01 (Figure 1A). This is consistent with previous reports showing that HLA-C peptide repertoires are generally smaller and less diverse than those of HLA-A and -B (Neisig et al., 1998; Rasmussen et al., 2014). The intermediate size of the HLA-B*46:01 peptidome is consistent with its binding site being a hybrid of the parental allotypes.

A majority (84.2%) of the peptides characterized is specific for one of the three HLAs, while only 15.8% bind to two of the three HLA class I molecules, and only one peptide, TSSYKPIV, binds all three (Figure 1A; Figure S1). Consistent with the similarity of their primary structures, the HLA-B*15:01 and HLA-B*46:01 peptidomes have the greatest overlap, with 333 shared peptides (Figure 1B). Although the sequences of the peptide-binding domains of HLA-B*15:01 and HLA-B*46:01 differ only by 3.8%, their peptidomes differ by >84%.

Consistent with their gene-specific polymorphisms (Turner et al., 1998; Zemmour and Parham, 1992), the peptide-binding domains of HLA-B*15:01 and HLA-C*01:02 differ by 14.4%, and these allotypes have only three peptides in common (Figure 1B). The peptide-binding domains of HLA-C*01:02 and HLA-B*46:01 differ by 10.6%, and these allotypes have 19 common peptides. Thus, the gene conversion that created HLA-B*46:01 gave it a new and distinctive peptidome.

The HLA-B*46:01 Peptidome Is Skewed toward Nonamer Peptides

We identified differences in the lengths of peptides bound by each allotype (Figure 1C). HLA-B*15:01-binding peptides exhibit a wide range in length: a minority (44%) are nonamer peptides and ~30% are longer than decamers (Figure 1D). With a majority (54%) of HLA-C*01:02-binding peptides being nonamers, their range is narrower than those of HLA-B*15:01 (Figure 1D, upper panel). HLA-B*46:01-binding peptides have the narrowest range, with >80% of them being nonamers or decamers (Figure 1D, upper panel). Among the 333 peptides shared by HLA-B*15:01 and B*46:01, ~75% are nonamers (Figure 1D, lower panel; Figure S1). Thus, the skewing of HLA-B*46:01 peptides for nonamers is more pronounced in peptides also bound by HLA-B*15:01. This contrasts with those shared with HLA-C*01:02, of which only 37% are nonamers (Figure 1D, lower panel). Thus, HLA-B*46:01 has a peptide-binding site with stronger selectivity for nonamer peptides than either parent.

HLA-B*46:01 Incorporates Elements from Both Parents in Its Peptide-Binding Motif

We next identified the amino acid preference of each peptidome. Peptides bound by HLA-B*15:01 and HLA-B*46:01 usually have Tyr, Phe, Leu, or Met at P9, and they share a similar, though less conserved, preference for Lys or Ile at P3. These properties are consistent with HLA-B*15:01 and HLA-B*46:01 having sequence identity in the F and D pockets that bind P9 and P3, respectively (Figure S1E).

By contrast, at P2, HLA-B*15:01 and HLA-B*46:01 have divergent preferences. Although both bind peptides with Leu at P2, Gln is abundant in HLA-B*15:01 peptides (26%) whereas Ala is most common in HLA-B*46:01 peptides (28%) (Figure 2A). Like HLA-B*46:01, HLA-C*01:02 binds peptides with Ala and Leu at P2 (32% and 17%, respectively), as well as peptides with Ser at P2 (20%). Thus, all three allotypes commonly bind peptides with Leu at P2, the most common amino acid in peptides bound by HLA-B*15:01, but not in those bound by HLA-B*46:01 or HLA-C*01:02 where Ala predominates. These results correlate

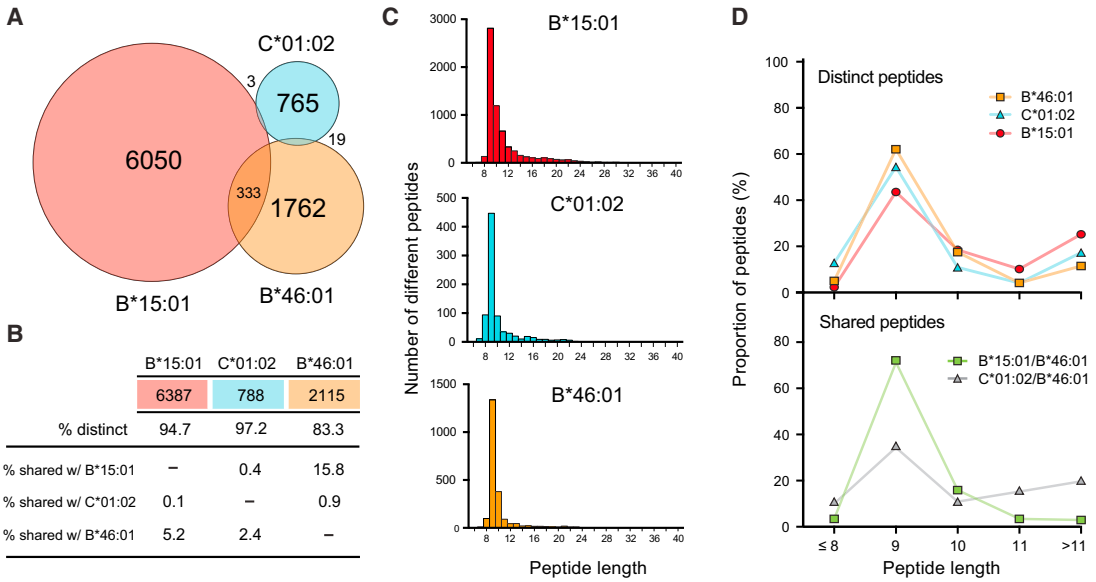

Figure 1. HLA-B*46:01, HLA-B*15:01, and HLA-C*01:02 Have Distinctive Peptidomes

(A) Venn diagram showing each peptidome represented by a color-shaded circle: HLA-B*15:01 (red), HLA-C*01:02 (blue), and HLA-B*46:01 (orange). The area of the circle is proportional to the number of distinct peptides (number shown in center of circle). The area of each circle overlap is proportional to the number of shared peptides (number shown within or beside each overlap) that bind to the two allotypes.

(B) Listed are the total number of peptides bound by HLA-B*15:01 (red), HLA-C*01:02 (blue), or HLA-B*46:01 (orange); the proportion bound by only that allotype (% distinct); as well as the proportion shared by pairs of allotypes (% shared with).

(C) For each allotype the histogram divides the binding peptides according to length, given as the number of amino acid residues.

(D) The proportion of peptides (%) that bind to one allotype (upper panel) or are shared by two allotypes (lower panel) plotted according to their length. The peptides shared by HLA-B*15:01 and HLA-C*01:02 are not plotted because they are too few.

with the sequences at positions 66–70 of the B pocket, which are identical in HLA-C*01:02 and HLA-B*46:01, but not in HLA-B*15:01 (Figure S1E). HLA-B*46:01 and HLA-C*01:02 share a common motif (Glu, Ala, or Ser) at position 8. This is an unexpected finding as the HLA backbone places limited constraint on P8 (Boyington et al., 2000). One possibility is that Val76, a residue shared by HLA-B*46:01 and HLA-C*01:02, mediates this effect. HLA-B*46:01 also acquired new properties in peptide selection. This is most evident at P1 where Phe and Tyr are common, but not in either parent (Figure 2A). The HLA*C*01:02 motif is different from the four broad motifs described for HLA-C (Rasmussen et al., 2014), in having Pro at P3 and Leu at P9 in >85% of its peptides.

Subsets of HLA-B*46:01-Binding Peptides Resemble HLA-B*15:01- or HLA-C*01:02-Binding Peptides

A covariation matrix was used to identify conserved pairs of amino acids in nonamer peptides bound by each allotype (Figure 2B). In the peptides bound by HLA-B*15:01 and HLA-B*46:01, pairs of residues at P2 and P9 are conserved. The most common motif observed in HLA-B*15:01 (~35%) and HLA-B*46:01 (~30%) peptides combines Leu at P2 with Tyr at P9. Both allotypes have a second, less common motif: Gln at P2 with Leu at P9 in HLA-B*15:01 and Ala at P2 with Leu at P9 in HLA-B*46:01 (Figure S2). For HLA-C*01:02 peptides, pairs of residues at P2 and P3 and at P3 and P9 are conserved. These peptides combine Ala at P2 with Pro at P3 and Pro at P3 with Leu at P9 (Figure S2C). Reflecting its hybrid structure, HLA-B*46:01- and HLA-B*15:01-binding peptides share the Leu2/Tyr9 9 pair of residues, whereas the HLA-B*46:01- and HLA-C*01:02-binding peptides share the Ala2/Leu9 pair of residues. Covariation between pairs of amino acid residues in peptides bound by MHC has been previously observed (Birnbaum et al., 2014), with structural analyses indicating it occurs due to alterations in the register of the peptide backbone, causing compensatory changes along the peptide-MHC interface (Chappell et al., 2015; Fremont et al., 1995; Koch et al., 2007).

Extending this analysis, we relaxed the requirement for conserved pairs of identical amino acids, and we compared the biochemical properties of each peptidome by principal-component analysis (PCA) (Figure 2C). The HLA-B*15:01 peptidome forms a single dominant cluster, contrasting with a small tight cluster formed by that of HLA-C*01:02. There is little spatial overlap between these peptidomes, indicating that they contain biochemically distinct peptides. The HLA-B*46:01 peptidome is more diffuse, resembling a fusion of the two parents. The larger cluster overlaps with that of HLA-B*15:01, the smaller one with HLA-C*01:02. These results are consistent with the covariation analysis (Figure 2B; Figure S2), and they show that HLA-B*46:01 presents two subsets of peptides that are biochemically similar, but not identical, to those of its parents.

A Minority of HLA-B*46:01 and HLA-C*01:02 Peptides Are Strong KIR2DL3 Ligands

HLA-B*46:01 and HLA-C*01:02, but not HLA-B*15:01, carry the C1 epitope and are recognized by KIR2DL3 (Moesta et al., 2008).

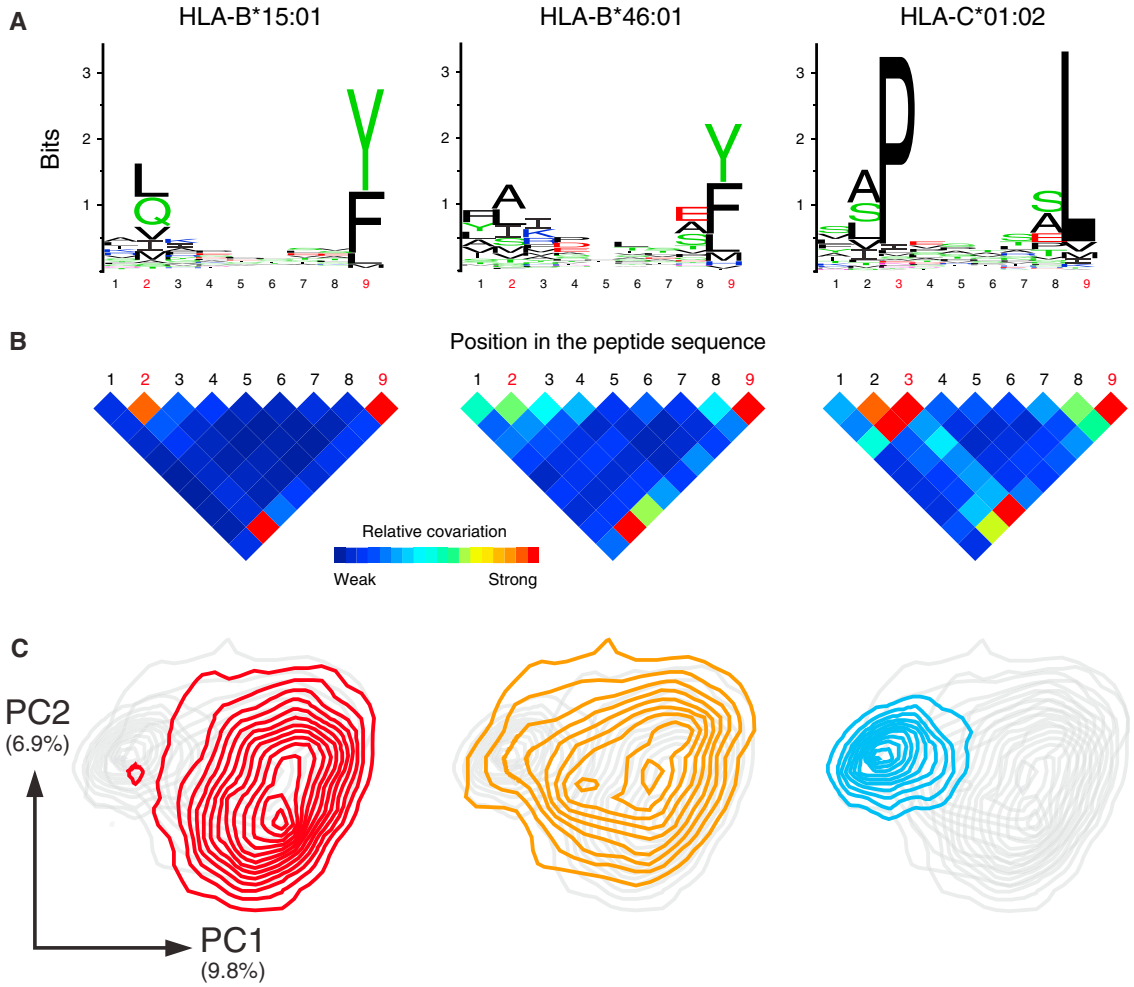

Figure 2. HLA-B*46:01 Binds a Subset of Peptides with a Distinctive Amino Acid Motif and Biochemical Properties

(A) Kullback-Leibler sequence logos showing amino acid preferences for nonamer peptides bound by HLA-B*15:01 (left), HLA-B*46:01 (center), and HLA-C*01:02 (right). Each logo consists of stacks of amino acid symbols, one stack for each position in the sequence. The total height of the column of amino acids represents the level of conservation at that position, and the residue height denotes its relative frequency. The colors of each amino acid correspond to their biochemical characteristics: acidic (red), basic (blue), hydrophobic (black), and polar (green). Sequence logos were generated using WebLogo (Crooks et al., 2004).

(B) Covariation matrices for nonamer peptides bound by each allotype. The color of each square represents the conservation at or covariation between the listed residues on a heatmap scale, with blue indicating weak covariation and red indicating strong covariation.

(C) PCA density plots show the distribution of nonamer peptides bound by HLA-B*15:01 (left, red), HLA-B*46:01 (center, orange), and HLA-C*01:02 (right, blue). For comparison, in each plot the distribution of nonamer peptides from the other allotypes is shown in gray. The percentage of the variation in the dataset shown by the first (PC1) and second (PC2) principal components is listed to the left.

To determine if KIR2DL3 displays a preference for specific peptide combinations, we incubated KIR2DL3-coated beads with sHLA, isolated the bound peptides, and determined their sequences by mass spectrometry. We call these peptides KIR permissive, as they enable the HLA molecule to be recognized by KIR2DL3.

No KIR-permissive peptides were isolated from HLA-B*15:01. By contrast, six KIR-permissive peptides were eluted from HLA-C*01:02 and 38 from HLA-B*46:01 (Figure S3). These peptides comprise 7% and 21% of the total number of peptides identified for HLA-C*01:02 and HLA-B*46:01, respectively (Figure 3A). For both allotypes, the proportion of nonamers was greater in KIR-permissive peptides (Figure 3B). That a higher proportion of HLA-B*46:01-binding peptides are KIR permissive is consistent with binding assays showing that HLA-B*46:01 has a higher affinity for KIR2DL3 than HLA-C*01:02 (Hilton et al., 2012, 2015a, 2015b; Moesta et al., 2008).

The sequences of the KIR-permissive and non-permissive nonamer peptides bound by HLA-B*46:01 were compared (Figure 3C). (The low number of KIR-permissive peptides identified precluded similar analysis of HLA-C*01:02.) KIR-permissive peptides have significantly increased frequency of Asn at P3 and Ser at P7 and decreased frequency of Glu at P7 and P8 (Figure 3D, upper panel). Analysis of the concatenated biochemical properties of peptides in each group showed significant differences only at the C terminus of the peptide (positions 7–9)

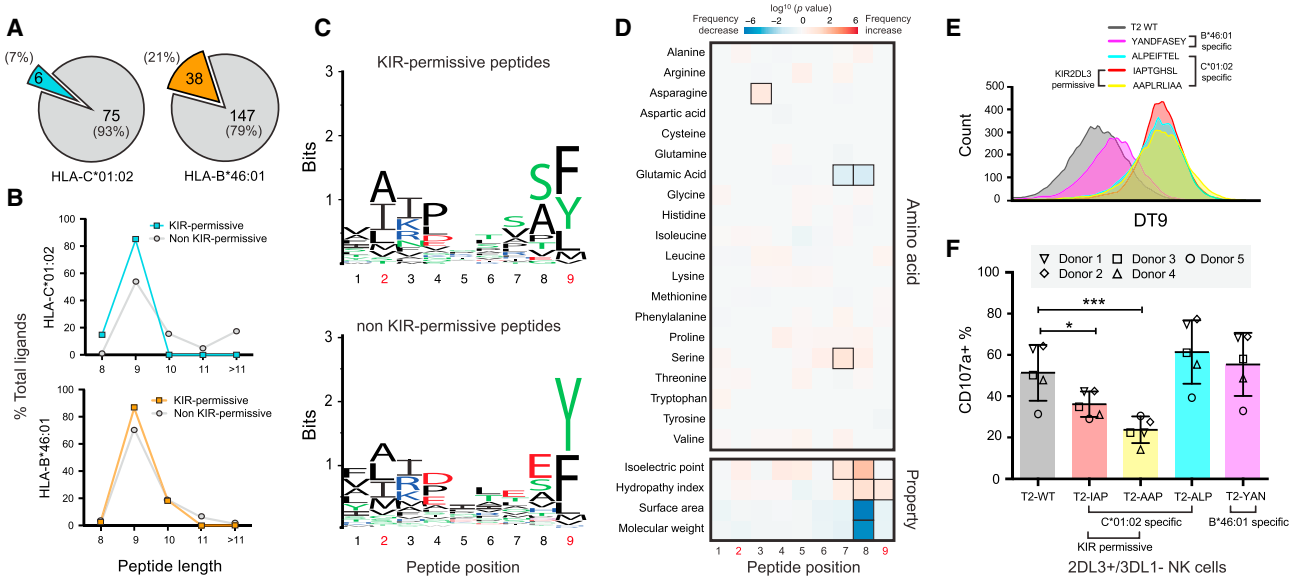

Figure 3. KIR2DL3 Recognition of HLA-B*46:01 and HLA-C*01:02 Is Peptide Dependent

(A) Pie charts showing the number and percentage of KIR2DL3-permissive peptides bound by HLA-C*01:02 (left, blue) and HLA-B*46:01 (right, orange) relative to non-permissive peptides (gray).

(B) The percentage of HLA-C*01:02 (blue, upper panel) and HLA-B*46:01 (orange, lower panel) peptides that are KIR permissive or non-permissive (gray) divided by length.

(C) Kullback-Leibler sequence logos representing the amino acid preferences for nonamer HLA-B*46:01 KIR-permissive (top panel) and non-permissive (bottom panel) peptides. The colors of each amino acid correspond to their biochemical characteristics: acidic (red), basic (blue), hydrophobic (black), and polar (green). Sequence logos were generated using WebLogo (Crooks et al., 2004).

(D) Heatmap matrix showing the $\log^{10}$ p values comparing the frequency of amino acids (top panel, Fisher's exact tests) and concatenated amino acid properties (bottom panel, two-sample t tests) between KIR-permissive and non-permissive peptides bound by HLA-B*46:01. Increases in the frequency of an amino acid or the value of a biochemical property are shown in red, decreases in blue. Amino acids or properties that differ significantly between the groups are outlined in black.

(E) Stabilization of HLA-C*01:02 expression on T2 cells as determined by DT9 staining (MFI shown on x axis) in the absence of peptide (wild-type) or with selected peptides pulsed at 100 μM and measured by flow cytometry. For (E) and (F), HLA allotype specificity and KIR2DL3 reactivity are indicated in the key.

(F) Degranulation of donor-derived KIR2DL3$^+$ NK cells incubated with T2 cells as determined by percentage CD107a expression in the absence of peptide (wild-type) or with selected peptides pulsed at 100 μM and measured by flow cytometry (bars represent mean ± SD). Horizontal lines indicate conditions in which degranulation differs significantly from wild-type (one-way ANOVA with multiple comparisons, *$p < 0.05$ and ***$p \leq 0.001$).

(Figure 3D, lower panel). Here, KIR-permissive peptides are significantly more likely to have small, positively charged, and hydrophobic amino acids.

KIR2DL3-Permissive Peptides Inhibit NK Cell Cytotoxicity

We next tested the capacity of KIR-permissive peptides to inhibit degranulation of NK cells. Donor-derived KIR2DL3$^+$ NK cells were tested for inhibition after incubation with TAP-deficient T2 cells (which naturally express HLA-C*01:02) loaded with selected peptides. Wild-type T2 cells with no exogenous peptide expressed low levels of HLA-C*01:02 (Figure 3E). KIR2DL3-expressing NK cells degranulated strongly when challenged with wild-type T2 cells (Figure 3F). Pulsing T2 cells with three HLA-C*01:02-specific peptides (two KIR permissive and one non-permissive) stabilized HLA-C*01:02 expression to a similar extent (Figure 3E). The HLA-B*46:01-specific peptide YANDFASEY stabilized HLA-C*01:02 expression but to a lesser degree (Figure 3E). Both KIR-permissive peptides significantly inhibited NK cell degranulation but to different degrees (Figure 3F). Consistent with their relative affinity for KIR2DL3 (Figure S3C), AAPLRLIAA (the higher affinity peptide) inhibited NK cell degranulation more than IAPTGHSL (Figure 3F). The non-permissive and HLA-B*46:01-specific peptides did not inhibit NK cell cytotoxicity (Figure 3F).

HLA-B*46:01 Has a Less Diverse Peptidome Than HLA-B*15:01

We performed two analyses to compare the diversity of each HLA peptidome. The relative sequence similarity of the amino acids in each peptidome was determined by calculating the per-position divergence in amino acid composition in five randomly selected sets of nonamer peptides. Consistent with previous studies of HLA-B and -C (Neisig et al., 1998; Rasmussen et al., 2014) and our analysis of the raw number of distinct peptides in each peptidome (Figure 1A), we found that the HLA-B*15:01 and HLA-C*01:02 peptidomes had the least and most sequence similarity, respectively, with the HLA-B*46:01 peptidome having intermediate sequence similarity (Figure 4A).

The true diversity of each peptidome was determined by comparing the abundance (intensity) of their bound peptides, as assessed by mass spectrometry. To control for the

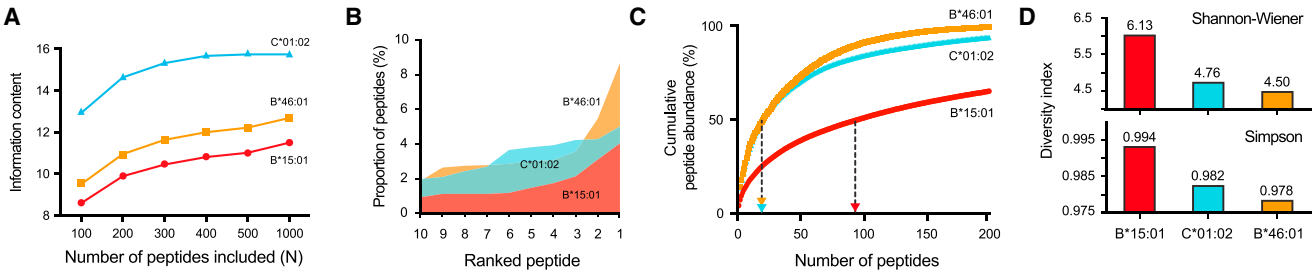

Figure 4. HLA-B*46:01 Has a Restricted Peptidome

(A) The information content of random subsets of N 9-mer peptides sampled from each allotype. For each value of N, this procedure was repeated 100 times and the mean is reported.

(B) For each allotype, the proportion of total peptides contributed by the ten most abundant peptides. The most abundant peptide is 1. The area under each plot is proportional to the percentage, from left to right, that the ten peptides contribute: HLA-B*15:01 (red), HLA-C*01:02 (blue), and HLA-B*46:01 (orange).

(C) Graph showing the cumulative peptide abundance (%), starting at 1 with the most abundant peptide and sequentially adding peptides of decreasing abundance. Arrows show the number of peptides that constitute 50% of the total peptidome.

(D) Histogram comparing the diversity of each peptidome as assessed by the Shannon-Wiener (upper panel) and Simpson (lower panel) diversity indices.

ionization potential of individual peptides, we only compared the distribution of the peptidomes. For HLA-B*15:01, HLA-C*01:02, and HLA-B*46:01, the ten most abundant peptides contribute 18%, 34%, and 37%, respectively, to the total peptide mass (Figure 4B; Figure S4). We next calculated the smallest number of peptides that account for 50% of the bound peptide mass. This number is 95 for HLA-B*15:01, 20 for HLA-C*01:02 and 20 for HLA-B*46:01 (Figure 4C; Figure S4). Thus, the HLA-B*15:01 peptidome has approximately five times the diversity of the HLA-C*01:02 and HLA-B*46:01 peptidomes. Calculation of diversity indices for each peptidome showed that HLA-B*15:01 is most diverse, followed by HLA-C*01:02 and then HLA-B*46:01 (Figure 4C). Together, these results show that HLA-B*46:01 has a smaller peptide repertoire that is less diverse in length, abundance, and amino acid content than its more closely related parent, and they highlight the formative effect of residues 66–76.

A Predictive Model Indicates that HLA-B*46:01 Differs from HLA-B*15:01 in Its Capacity to Bind Pathogen-Derived Peptides

HLA class I peptidomes with low diversity are thought to provide protection against one or a number of closely related pathogens (Chappell et al., 2015). Epidemiologic studies suggest that the *HLA-B*46:01-MICA-A5* haplotype protects against development of lepromatous leprosy, the fulminant form of disease caused by *M. leprae* (Wang et al., 1999). Leprosy is endemic to Southeast Asia, where *HLA-B*46:01* is found at high frequency (Figures 5A and 5B) (González-Galarza et al., 2015). We hypothesized that HLA-B*46:01 might be better adapted to present peptide antigens derived from *M. leprae* than one or both of its parents. To assess this possibility, we identified 22 antigenic *M. leprae* proteins (Wiker et al., 2011), and we used a nine-amino acid-sliding window to create a library of all possible nonamer peptides. Their binding to each allotype was predicted using NetMHC 4.0 (retrained to include data from this study) (Nielsen et al., 2003).

In support of our hypothesis, HLA-B*46:01 is predicted to bind a significantly higher number of *M. leprae*-derived peptides than HLA-B*15:01 (Figure 5C; Figure S5). HLA-C*01:02 also presents a higher number of *M. leprae*-derived peptides, although the difference is not significant. Similarly, both HLA-B*46:01 and HLA-C*01:02 are predicted to bind a significantly higher number of *Mycobacterium tuberculosis*-derived peptides than HLA-B*15:01 (Figure 5C). By contrast, HLA-B*46:01 binds equal or lower numbers of peptides derived from *Salmonella* Enteritidis, HIV-1, or H1N1-influenza as compared to its parents (Figure 5D). This decrease is significant for HIV-1-derived peptides (Figure 5C).

We compared the distribution of the *M. leprae*-derived peptides predicted to bind HLA-B*46:01 to the distribution of the empirically determined peptides (shown in Figure 2C, center panel). To assess their relative similarity to the HLA-C*01:02-like and HLA-B*15:01-like peptides, we used k-nearest neighbor clustering to define two discontinuous subsets. When divided in this way, 15% of HLA-B*46:01 peptides fall in HLA-C*01:02-like cluster 1 and 85% of peptides fall in HLA-B*15:01-like cluster 2 (Figure 5E, top panel). Comparison with *M. leprae*-derived peptides predicted to bind HLA-B*46:01 shows a significantly higher percentage (25%) fall in HLA-C*01:02-like cluster 1 (Figure 5E). This shift to the C*01:02-like cluster 1 is also noted in KIR-permissive peptides that are more than twice as likely to fall in cluster 1 (33%) as compared to the wider HLA-B*46:01 peptidome. Together these results suggest that HLA-B*46:01 may provide protection against lepromatous leprosy because it is better adapted to present *M. leprae*-derived peptide antigens for immunosurveillance by NK cells and $CD8^+$ T cells.

DISCUSSION

This study defines at high resolution the peptidomes of HLA-B*46:01 and its parent allotypes. The HLA-B*46:01 peptidome is restricted in the length, type, and frequency of peptides that it presents for immunosurveillance. A minority of peptides bound by HLA-B*46:01 and HLA-C*01:02 form ligands for the NK cell receptor KIR2DL3. HLA-B*46:01 is significantly better adapted than its more closely related parent HLA-B*15:01 to bind antigenic peptides derived from *M. leprae.* These distinctive functions are consistent with a model in which HLA-B*46:01 rose

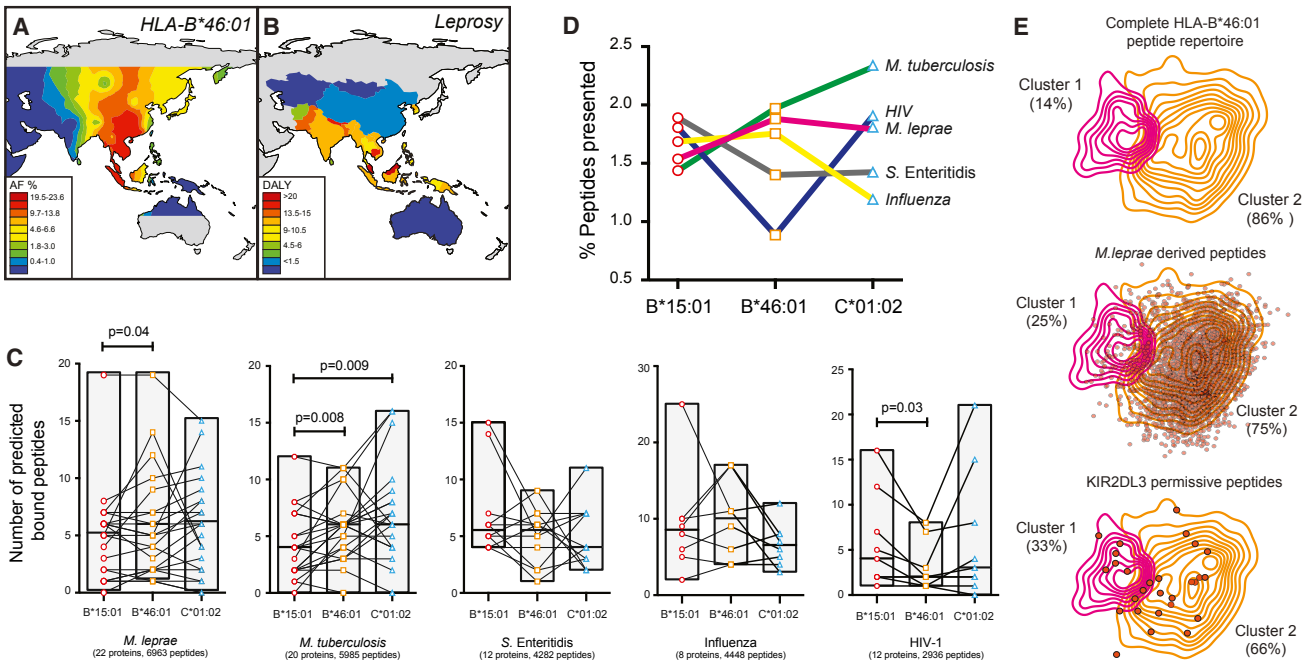

Figure 5. HLA-B*46:01 Differs from HLA-B*15:01 in Its Capacity to Bind Pathogen-Derived Peptides

(A) Inverse distance weighted map (ArcGIS) showing frequency of *HLA-B*46:01* in Southeast Asia. Color scale bars correspond to allele frequency categories. Frequencies are from allelefrequencies.net (González-Galarza et al., 2015).

(B) Map showing the disability life-adjusted life year (DALY) for leprosy per 100,000 inhabitants of Southeast Asia (Mathers et al., 2008). Disability life-adjusted life year is a measure of overall disease burden, expressed as the number of years lost due to disability, ill health, or early death.

(C) Plots representing the number of nonamer peptides derived from *Mycobacterium leprae*, *Mycobacterium tuberculosis*, *Salmonella* Enteritidis, H1N1 influenza, and HIV-1 predicted to bind each allotype. The median of each plot is indicated with a solid black line. Red circles (HLA-B*15:01), orange squares (HLA-B*46:01), and blue triangles (HLA-C*01:02) linked with black lines indicate the number of peptides derived from each antigenic protein predicted to bind the given allotype. Listed below each plot is the total number of proteins and peptides investigated. Horizontal bars with associated p values (paired t tests) indicate significant differences. Binding predictions were made using NetMHC 4.0 (Nielsen et al., 2003).

(D) Summary plot showing the percentage of pathogen-derived peptides bound by each allotype.

(E) Principal-component analysis density plot showing the distribution of nonamer peptides bound by HLA-B*46:01, divided into two clusters (HLA-C*01:02-like, pink; B*15:01-like, orange) on the basis of a k-nearest neighbor algorithm (top panel). The distribution of *M. leprae*-derived peptides predicted to bind HLA-B*46:01 (center panel, red dots) and KIR2DL3-permissive peptides bound by HLA-B*46:01 (bottom panel, red dots) is shown overlaid on the HLA-B*46:01 peptidome, with the percentage of peptides falling in each cluster shown. *M. leprae*-derived peptides are significantly more likely to fall in cluster 1 (Fisher's exact test, p = 0.0028).

in frequency in Southeast Asia because it provides carriers with protection from severe leprosy.

HLA-B*15:01 and HLA-B*46:01 share Ser77 and Asn80, the residues commonly associated with the C1 epitope. However, these residues are insufficient to confer reactivity with KIR2DL3 without HLA-C*01:02-derived Val76. We show that the interaction between KIR2DL3 and HLA is dependent on the length and sequence of the bound peptide. Consistent with previous studies using exogenous peptide, we found that KIR recognition of endogenously processed peptides was most sensitive to the amino acid at position 8 and more generally to those at the C terminus of the peptide, a region that corresponds to the KIR-binding site (Boyington et al., 2000). Although no structure of KIR2DL3 in complex with its ligand has been solved, comparison with KIR2DL2 bound to HLA-C*03:04 shows that Gln71 in the D1 domain forms a hydrogen bond with the amino acid at P8 (Boyington et al., 2000). The formation of this hydrogen bond brings Gln71, Ser184, and Glu187 of KIR2DL2 (residues that are identical in KIR2DL3) into such close proximity with the peptide that it constrains the size of the P8 side chain that would allow interaction with KIR. KIR2DL2 also directly contacts the amino acid at position 7 in the peptide, which is more exposed in this structure as compared to other HLA class I (Fan et al., 2001). Interestingly, we identified one peptide, the nonamer YANDFASEY, that bound KIR2DL3 despite having Glu at P8. This finding indicates that, despite a general preference for peptides with small size and low hydrophobicity and specifically for those without Glu at P8, KIR2DL3 is able to recognize selected peptides with these characteristics. Additional functional experiments are needed to confirm this finding. Furthermore, we found that Asn at P3 is significantly more common in KIR2DL3-permissive peptides, indicating that residues outside the KIR-binding site may also influence recognition of HLA-B*46:01 by KIR2DL3, presumably as a result of structural constraints imposed through the peptide backbone.

Although less stringent than the interaction between the CD8 TCR and HLA (Malnati et al., 1995), our data suggest that the majority of peptides (>75%) presented by HLA-B*46:01 and

HLA-C*01:02 do not provide strong ligands for KIR2DL3. Similarly, a previous study showed that KIR2DL3 recognized only a small number of exogenous peptides bound by HLA-C*08:02 (Sim et al., 2017). This specificity may explain why KIR2DL3 binding to C1 appears weaker than that of KIR2DL2 to C1 or KIR2DL1 to C2 (Hilton et al., 2012, 2015a; Moesta et al., 2008). A second implication of this specificity is that the system may be usurped by pathogens. Supporting this possibility, previous studies have shown that HIV produces escape mutants (Alter et al., 2011; Hölzemer et al., 2015). One example is a mutation in the p24 Gag epitope that enabled significantly better binding of KIR2DL3 to HLA-C*03:04-expressing cells presenting the variant epitope (Hölzemer et al., 2015). Antagonism of NK cell function by peptides with weak affinity for KIR is likely to be another functional consequence of KIR2DL3 peptide selectivity. Although the specific molecular mechanisms that underlie the effect are unclear, peptides with weak affinity for inhibitory KIR antagonize those with high affinity, preventing inhibitory synapse formation and reducing the inhibitory signaling potential of NK cells (Borhis et al., 2013; Fadda et al., 2010). Previous estimates indicate ~30% of HLA-C*01:02-bound peptides provide strong ligands for KIR2DL2 and 2DL3 (Fadda et al., 2010). We find that only 7% of HLA-C*01:02-bound peptides and 21% of HLA-B*46:01-bound peptides provide strong ligands for KIR2DL3, suggesting that peptide antagonism may play a greater functional role than previously recognized.

The HLA-B*46:01 peptidome is smaller and less diverse than that of HLA-B*15:01, its more closely related parent. This loss of diversity may result from reduced plasticity of the HLA-C*01:02-derived α_1 helix segment that restricts the range of permissible peptides (Sibilio et al., 2005, 2008). A basic patch comprising R62, K66, and R69 may contribute further restriction. These residues likely contribute to the shared preference of HLA-C*01:02 and HLA-B*46:01 for acidic residues at position 4 and the additional length and frequency constraints that differentiate these allotypes from HLA-B*15:01 (Barber et al., 1996).

In addition to its effect on the plasticity of the peptide-binding groove, the HLA-C*01:02-derived α_1 helix segment contains the KYRV motif, which reduces cell-surface expression of HLA-C relative to HLA-A and -B (Sibilio et al., 2008). Although the cell-surface expression of HLA-B*46:01 has not specifically been studied, it is known to have increased intracellular retention due to prolonged association with HLA-dedicated chaperones (Sibilio et al., 2008). Thus, HLA-B*46:01 likely combines low-cell-surface expression with a low-diversity peptidome. By contrast, several studies have demonstrated an inverse correlation between cell-surface expression and peptidome diversity (Chappell et al., 2015; Tregaskes et al., 2016). First described in the chicken MHC, an initial survey of four HLA-B allotypes shows a similar correlation, suggesting it is a broadly conserved feature (Chappell et al., 2015). Thus, HLA-B*46:01 appears an outlier in this regard and more characteristic of HLA-C than HLA-B. The relationship between cell-surface expression and peptidome diversity within HLA-C has not been extensively studied, although HLA-C allotypes are known to exhibit differential cell-surface expression (Apps et al., 2013).

Comparative studies have shown that MHC class I with restricted peptidomes confer protection against one or several closely related pathogens, whereas those with more diverse peptidomes confer broader disease resistance (Chappell et al., 2015; Tregaskes et al., 2016). In the former category, HLA-B*46:01 may permit prioritization of peptides from a specific pathogen, allowing an individual to mount an effective immune response. One candidate pathogen is *M. leprae* that causes leprosy, a chronic granulomatous infection of the skin and peripheral nerves. Leprosy emerged as a major infectious disease in the last 50,000 years as modern humans expanded outward across the globe from Africa (Monot et al., 2005). Infection rates likely peaked with the mass movement of people along trade routes between Africa and Asia prior to the advent of modern medicine (Karlsson et al., 2014). Leprosy is still common in many tropical regions, Southeast Asia being a notable hotbed of the disease (Reibel et al., 2015). Leprosy has exerted strong selective pressure on the human genome in general (Karlsson et al., 2014) and on the *HLA* region in particular (Chan, 1983; Franceschi et al., 2011; Shankarkumar, 2004; Shankarkumar et al., 2003; Takata et al., 1978; Zhang et al., 2009).

Epidemiologic studies show that carriers of the *HLA-B*46:01-MICA-A5* haplotype are protected against the development of lepromatous leprosy, the fulminant, life-threatening form of the disease (Wang et al., 1999). Consistent with this finding, we show that HLA-B*46:01 is predicted to bind a significantly higher number of antigenic peptides derived from *M. leprae* than its parent allotype HLA-B*15:01 and a similar number to that bound by HLA-C*01:02. Because *HLA-B*46:01* and *HLA-C*01:02* are in strong linkage disequilibrium (Abi-Rached et al., 2010), the result is that *HLA-B*46:01* carriers would have at least two *HLA class I* loci able to effectively present *M. leprae*-derived peptides. Presentation of *M. leprae* peptides to the TCR and KIR cells is likely to result in a strong cell-mediated immune response, which is a major determining factor in the clinical progression of leprosy (Kaleab et al., 1995; Ridley, 1974). Supporting a role for KIR-mediated immunity in the outcome of *M. leprae* infection, studies show that patients with the less severe tuberculoid form of leprosy have increased frequencies of activating KIR2DS2 and KIR2DS3 (Franceschi et al., 2008). Together these findings support the hypothesis that *HLA-B*46:01* rose in frequency because it confers protection against severe infection caused by *M. leprae.*

Arguing against this mechanism is our finding that both HLA-B*46:01 and HLA-C*01:02 present a higher number of peptides derived from *M. tuberculosis*. In contrast to leprosy, an epidemiologic study shows that *HLA-B*46:01* carriers are more susceptible to pulmonary tuberculosis (Chandanayingyong et al., 1988). Although this study was small (only 36 subjects) and susceptibility was also linked to *HLA class II*, it suggests that the number of pathogen-derived peptides bound by a given allotype may not be the dominant mechanism that promotes disease resistance.

Intense reactivity against pathogens and a lack of collateral reactivity to self are critical features of a successful immune system. HLA-B*46:01 appears able to succeed in the first requirement (although apparently with a narrow remit as epidemiologic studies show it confers susceptibility to tuberculosis, malaria, HIV, and SARS coronavirus; Chandanayingyong et al., 1988; Hananantachai et al., 2005; Huang et al., 2009; Lin et al.,

2003). However, several studies suggest that it falls short in the second, predisposing individuals to autoimmune conditions, including myasthenia gravis (Chan et al., 1993) and Graves disease (Chan et al., 1978; Hawkins et al., 1985; Naito et al., 1987), as well as to nasopharyngeal carcinoma (Chan et al., 1983). The apparent predisposition to self-reactivity may occur because of reduced TCR diversity (a likely result of its low-diversity peptidome), increased NK cell reactivity, or an as yet undiscovered mechanism. However, these data support the notion that there is an immunological trade-off between protection against infectious disease and protection against self-reactivity. Intriguingly, this hypothesis is consistent with the clinical observation that patients with psoriasis, an autoimmune skin condition, are protected from the development of leprosy (Dogra et al., 2003; Hensler and Christophers, 1995; Wahba et al., 1980).

EXPERIMENTAL PROCEDURES

Further details are given in the Supplemental Experimental Procedures.

Isolation of HLA Class I Complexes from 721.221 Cells

Isolation and analysis of peptides were performed as previously described (McMurtrey et al., 2016; Trolle et al., 2016; Yaciuk et al., 2014). Briefly, 721.221 cells, which lack endogenous HLA class I expression, were transfected with constructs encoding soluble forms (sHLA) of HLA-B*15:01, HLA-B*46:01, and HLA-C*01:02. sHLA binds a similar peptide repertoire to membrane-associated HLA class I (Scull et al., 2012). The sHLA-peptide complexes were affinity purified from the cell supernatant on an anti-W6/32 Sepharose column, eluted, and the bound peptides dissociated from the HLA by denaturation in 10% acetic acid for 15 min at 75°C. Peptides were separated from the denatured proteins by passage through a stirred cell ultrafiltration device (3-kDa-cutoff membrane [Millipore]). The peptide-containing filtrate was lyophilized, re-suspended in 10% acetic acid, and separated into ~40 fractions by reverse-phase high-performance liquid chromatography (HPLC) as described (Trolle et al., 2016). Each fraction was dried and re-suspended in 10% acetic acid for liquid chromatography-mass spectrometry (LC-MS). Approximately 25% of each HPLC fraction was injected into a nano-scale reverse-phase liquid chromatography Eksigent nano-LC-4000 (Sciex) system. Column specifications, mobile phase solvents, and the elution gradient were as described (Trolle et al., 2016). Eluted fractions were ionized using a NanoSpray III (Sciex) ion source into a Sciex TripleTOF 5600 mass spectrometer.

Isolation and Analysis of KIR-Permissive Peptide Ligands from 721.221 Cells

Biotinylated KIR2DL3 monomer was incubated with streptavidin-coated microbeads (Thermo Fisher Scientific), according to the manufacturer's instructions, and washed to remove excess KIR2DL3. Then 300 μl containing 75 μg W6/32-purified sHLA-B*15:01, sHLA-C*01:02, and sHLA-B*46:01 material was divided into three equal aliquots each and incubated for 16 hr at 4°C with KIR2DL3-conjugated microbeads, unconjugated blank beads, or no beads. KIR2DL3-conjugated beads were added in 3.5 molar excess of KIR2DL3 to sHLA. Following incubation, each 25-μg aliquot was washed with 30 bead volumes, and ligand identification was performed in data-independent mode (DIA) in triplicate.

NK Cell Cytotoxicity Assay Using T2 Cell Lines

To test the effect of specific peptides, T2 cells were incubated in serum-free RPMI media overnight at 26°C in the presence of 100 μM synthetic peptide (GenScript). Cells were washed and stained with the HLA-C-specific DT9 antibody (EMD Millipore). Peptide stabilization was assessed by flow cytometry on an Accuri C6 benchtop flow cytometer (BD Biosciences).

NK cells were isolated from five healthy *KIR A haplotype* and *HLA-C1* homozygous donors, and they were stimulated overnight with 500 units/mL recombinant human IL-2 (R&D Systems) in RPMI 10% complete media. T2 cells (3×10^4) were incubated with 100 μM peptide (Genscript) overnight in serum-free media at 26°C, washed, and re-suspended in serum-free media with anti-CD107a-TexasRed antibody (eBioscience). T2 cells were incubated with NK cells at a target:effector ratio of 10:1 for 3.5 hr in serum-free media with 500 units/mL recombinant human IL-2. Surface staining was performed using anti-KIR2DL2/3-APC GL183 (Beckman Coulter) and anti-KIR3DL1-FITC DX9 (BioLegend) to identify $KIR2DL3^+/KIR3DL1^-$ NK cells. Following surface staining, cells were treated with live/dead orange (Life Sciences) and fixed (Cytofix, BD Biosciences). Cells were analyzed on an LSR II cytometer (BD Biosciences) at the Stanford Flow Cytometry Core Facility. A representative gating strategy is shown in Figure S5B.

Statistical and Bioinformatic Methods

Calculation of Peptidome Sequence Similarity

The information content for each peptidome was calculated as the summed Kullback-Leibler distance (KLD) over the positions in the binding motif. A random subset of N 9-mer peptides was sampled from each allotype, and amino acids frequencies (p_{aa}) were estimated using sequence weighting and pseudo counts correction for a low number of observations, as previously described (Nielsen et al., 2004). The KLD at each position was calculated as sum $2^* p_{aa} * \log2(p_{aa}/q_{aa})$, where q_{aa} is the background frequency of amino acid (aa). For each value of N, this procedure was repeated 100 times and the mean is reported.

Covariation Analysis

To search for covariation between peptide positions, coupling terms were calculated as described (Lockless and Ranganathan, 1999) and plotted as a heatmaps, processed and analyzed with custom Perl and MATLAB (MathWorks) scripts as described (Mendoza et al., 2012). Scripts are available upon request.

PCA

For each amino acid in a peptide, four biochemical properties (molecular weight, hydropathy index, surface area, and isoelectric point) were determined. Thus, 36 variables were generated for each nonamer peptide. A custom R script (available at www.stanford.edu/group/parhamlab/software) was used to generate PCA plots for nonamer peptides from the three HLA class I allotypes. The k-nearest neighbor algorithm (k = 15) (Venables and Ripley, 2002) was used to cluster the HLA-B*46:01 peptidome by similarity to those of HLA-B*15:01 and HLA-C*01:02. Comparison of the distribution of empirically determined HLA-B*46:01 peptides to either *M. leprae*-derived peptides predicted to bind HLA-B*46:01 or HLA-B*46:01 KIR-permissive peptides was made using a Fisher's exact test.

Analysis of KIR-Permissive versus Non-permissive Peptides

Fisher's exact (specific amino acids) and two sample t tests (concatenated properties) were used to determine the magnitude of frequency changes at each position of the peptide between KIR-permissive and non-permissive groups.

NK Cell Degranulation Assay

One-way ANOVA tests with multiple comparisons were used to quantify the magnitude of changes in NK cell degranulation (percentage CD107a expression) between KIR-permissive and non-permissive peptides bound by HLA-C*01:02.

*Prediction of Pathogen-Derived Peptide Binding to HLA-B*15:01, HLA-B*46:01, and HLA-C*01:02*

A literature search identified a set of antigenic proteins derived from five pathogens: *M. leprae* (taken from Table 2 in Wiker et al., 2011), *M. tuberculosis* (taken from Table 1 in Målen et al., 2008), *S.* Enteritidis (taken from Table 3 in Cho et al., 2015), and the complete proteome of HIV-1 (Doherty et al., 2005) and H1N1 influenza A, strain PR1934 (NIAID Influenza Genome Sequencing Consortium, www.fludb.org). A nine-amino acid-sliding window was used to create a library of all possible nonamer peptides from each protein, and their binding to each allotype was predicted with NetMHC 4.0 (Nielsen et al., 2003). The model used to make these predictions was trained on 436 nonamer peptides and 2,180 random natural negative nonamer peptides using the NNAlign method (Andreatta et al., 2011). Percentile rank scores were estimated from the distribution of prediction scores of 100,000 random natural 9-mer peptides. Peptides were considered to bind if their predicted percentile

score was ≤2%. Paired t tests were used to compare the number of peptides bound by HLA pairs.

All statistical calculations were performed in GraphPad Prism 6.0 with $\alpha = 0.05$.

SUPPLEMENTAL INFORMATION

Supplemental Information includes Supplemental Experimental Procedures and five figures and can be found with this article online at http://dx.doi.org/10.1016/j.celrep.2017.04.059.

AUTHOR CONTRIBUTIONS

Conceptualization, H.G.H. and C.P.M.; Methodology, H.G.H., C.P.M., A.S.H., Z.D., J.H.B., A.G., A.H., and M.N.; Software, A.S.H., J.L.M., and M.N.; Investigation, H.G.H., C.P.M., Z.D., J.L.P., R.B., W.B., and K.W.J.; Resources, D.A.B., P.J.R., M.E.B., K.C.G., W.H.H., and P.P.; Data Curation, H.G.H., C.P.M., A.S.H., J.L.M., and M.N.; Acquisition of Data, H.G.H., C.P.M., A.S.H., R.B., W.B., and K.W.J.; Writing – Original Draft, H.G.H. and P.P.; Writing – Review & Editing, H.G.H., L.A.G., and P.P.; Funding Acquisition, H.G.H., L.A.G., and P.P.; Supervision, K.C.G., W.H.H., and P.P.

ACKNOWLEDGMENTS

Major funding for this work was provided by NIH grant R01 AI22039 to P.P. A.S.H. is supported by the Stanford Developmental Biology and Genetics training grant NIH 5 T32 GM007790. J.L.P. is supported by the Stanford Immunology postdoctoral training grant to Molecular and Cellular Immunobiology, 5 T32 AI07290, NIH National Institute of Allergy and Infectious Diseases (NIAID). J.L.M. is supported by NIH award K01CA175127. Further funding was provided by the Emergent Technologies Innovation Fund to W.H.H. and NIH grants 5R01 AI103867 and 1U1 AI057229 to K.C.G., who is also supported by Howard Hughes Medical Institute (HHMI). The funders had no role in study design, data collection or analysis, decision to publish, or preparation of the manuscript.

Received: October 10, 2016
Revised: March 7, 2017
Accepted: April 20, 2017
Published: May 16, 2017

REFERENCES

Abi-Rached, L., Moesta, A.K., Rajalingam, R., Guethlein, L.A., and Parham, P. (2010). Human-specific evolution and adaptation led to major qualitative differences in the variable receptors of human and chimpanzee natural killer cells. PLoS Genet. *6*, e1001192.

Alter, G., Heckerman, D., Schneidewind, A., Fadda, L., Kadie, C.M., Carlson, J.M., Oniangue-Ndza, C., Martin, M., Li, B., Khakoo, S.I., et al. (2011). HIV-1 adaptation to NK-cell-mediated immune pressure. Nature *476*, 96–100.

Andreatta, M., Schafer-Nielsen, C., Lund, O., Buus, S., and Nielsen, M. (2011). NNAlign: a web-based prediction method allowing non-expert end-user discovery of sequence motifs in quantitative peptide data. PLoS ONE *6*, e26781.

Apps, R., Qi, Y., Carlson, J.M., Chen, H., Gao, X., Thomas, R., Yuki, Y., Del Prete, G.Q., Goulder, P., Brumme, Z.L., et al. (2013). Influence of HLA-C expression level on HIV control. Science *340*, 87–91.

Barber, L.D., Percival, L., Valiante, N.M., Chen, L., Lee, C., Gumperz, J.E., Phillips, J.H., Lanier, L.L., Bigge, J.C., Parekh, R.B., and Parham, P. (1996). The inter-locus recombinant HLA-B*4601 has high selectivity in peptide binding and functions characteristic of HLA-C. J. Exp. Med. *184*, 735–740.

Barreiro, L.B., and Quintana-Murci, L. (2010). From evolutionary genetics to human immunology: how selection shapes host defence genes. Nat. Rev. Genet. *11*, 17–30.

Biassoni, R., Falco, M., Cambiaggi, A., Costa, P., Verdiani, S., Pende, D., Conte, R., Di Donato, C., Parham, P., and Moretta, L. (1995). Amino acid substitutions can influence the natural killer (NK)-mediated recognition of HLA-C molecules. Role of serine-77 and lysine-80 in the target cell protection from lysis mediated by "group 2" or "group 1" NK clones. J. Exp. Med. *182*, 605–609.

Birnbaum, M.E., Mendoza, J.L., Sethi, D.K., Dong, S., Glanville, J., Dobbins, J., Ozkan, E., Davis, M.M., Wucherpfennig, K.W., and Garcia, K.C. (2014). Deconstructing the peptide-MHC specificity of T cell recognition. Cell *157*, 1073–1087.

Borhis, G., Ahmed, P.S., Mbiribindi, B., Naiyer, M.M., Davis, D.M., Purbhoo, M.A., and Khakoo, S.I. (2013). A peptide antagonist disrupts NK cell inhibitory synapse formation. J. Immunol. *190*, 2924–2930.

Boyington, J.C., Motyka, S.A., Schuck, P., Brooks, A.G., and Sun, P.D. (2000). Crystal structure of an NK cell immunoglobulin-like receptor in complex with its class I MHC ligand. Nature *405*, 537–543.

Chan, S.H. (1983). HLA and skin disease in the Chinese. Ann. Acad. Med. Singapore *12*, 3–5.

Chan, S.H., Yeo, P.P., Lui, K.F., Wee, G.B., Woo, K.T., Lim, P., and Cheah, J.S. (1978). HLA and thyrotoxicosis (Graves' disease) in Chinese. Tissue Antigens *12*, 109–114.

Chan, S.H., Day, N.E., Kunaratnam, N., Chia, K.B., and Simons, M.J. (1983). HLA and nasopharyngeal carcinoma in Chinese–a further study. Int. J. Cancer *32*, 171–176.

Chan, S.H., Tan, C.B., Lin, Y.N., Wee, G.B., Degli-Esposti, M.A., and Dawkins, R.L. (1993). HLA and Singaporean Chinese myasthenia gravis. Int. Arch. Allergy Immunol. *101*, 119–125.

Chandanayingyong, D., Maranetra, N., and Bovornkitti, S. (1988). HLA antigen profiles in Thai tuberculosis patients. Asian Pac. J. Allergy Immunol. *6*, 77–80.

Chappell, P., Meziane, K., Harrison, M., Magiera, Ł., Hermann, C., Mears, L., Wrobel, A.G., Durant, C., Nielsen, L.L., Buus, S., et al. (2015). Expression levels of MHC class I molecules are inversely correlated with promiscuity of peptide binding. eLife *4*, e05345.

Cho, Y., Park, S., Barate, A.K., Truong, Q.L., Han, J.H., Jung, C.H., Yoon, J.W., Cho, S., and Hahn, T.W. (2015). Proteomic analysis of outer membrane proteins in Salmonella enterica Enteritidis. J. Microbiol. Biotechnol. *25*, 288–295.

Colonna, M., and Samaridis, J. (1995). Cloning of immunoglobulin-superfamily members associated with HLA-C and HLA-B recognition by human natural killer cells. Science *268*, 405–408.

Crooks, G.E., Hon, G., Chandonia, J.M., and Brenner, S.E. (2004). WebLogo: a sequence logo generator. Genome Res. *14*, 1188–1190.

Dogra, S., Kaur, I., and Kumar, B. (2003). Leprosy and psoriasis: an enigmatic relationship. Int. J. Lepr. Other Mycobact. Dis. *71*, 341–344.

Doherty, R.S., De Oliveira, T., Seebregts, C., Danaviah, S., Gordon, M., and Cassol, S. (2005). BioAfrica's HIV-1 proteomics resource: combining protein data with bioinformatics tools. Retrovirology *2*, 18.

Fadda, L., Borhis, G., Ahmed, P., Cheent, K., Pageon, S.V., Cazaly, A., Stathopoulos, S., Middleton, D., Mulder, A., Claas, F.H., et al. (2010). Peptide antagonism as a mechanism for NK cell activation. Proc. Natl. Acad. Sci. USA *107*, 10160–10165.

Fan, Q.R., Long, E.O., and Wiley, D.C. (2001). Crystal structure of the human natural killer cell inhibitory receptor KIR2DL1-HLA-Cw4 complex. Nat. Immunol. *2*, 452–460.

Franceschi, D.S., Mazini, P.S., Rudnick, C.C., Sell, A.M., Tsuneto, L.T., de Melo, F.C., Braga, M.A., Peixoto, P.R., and Visentainer, J.E. (2008). Association between killer-cell immunoglobulin-like receptor genotypes and leprosy in Brazil. Tissue Antigens *72*, 478–482.

Franceschi, D.S., Tsuneto, L.T., Mazini, P.S., Sacramento, W.S., Reis, P.G., Rudnick, C.C., Clementino, S.L., Sell, A.M., and Visentainer, J.E. (2011). Class-I human leukocyte alleles in leprosy patients from Southern Brazil. Rev. Soc. Bras. Med. Trop. *44*, 616–620.

Fremont, D.H., Stura, E.A., Matsumura, M., Peterson, P.A., and Wilson, I.A. (1995). Crystal structure of an H-2Kb-ovalbumin peptide complex reveals the interplay of primary and secondary anchor positions in the major histocompatibility complex binding groove. Proc. Natl. Acad. Sci. USA *92*, 2479–2483.

Garboczi, D.N., Ghosh, P., Utz, U., Fan, Q.R., Biddison, W.E., and Wiley, D.C. (1996). Structure of the complex between human T-cell receptor, viral peptide and HLA-A2. Nature *384*, 134–141.

González-Galarza, F.F., Takeshita, L.Y., Santos, E.J., Kempson, F., Maia, M.H., da Silva, A.L., Teles e Silva, A.L., Ghattaoraya, G.S., Alfirevic, A., Jones, A.R., and Middleton, D. (2015). Allele frequency net 2015 update: new features for HLA epitopes, KIR and disease and HLA adverse drug reaction associations. Nucleic Acids Res. *43*, D784–D788.

Guethlein, L.A., Norman, P.J., Hilton, H.G., and Parham, P. (2015). Co-evolution of MHC class I and variable NK cell receptors in placental mammals. Immunol. Rev. *267*, 259–282.

Hananantachai, H., Patarapotikul, J., Ohashi, J., Naka, I., Looareesuwan, S., and Tokunaga, K. (2005). Polymorphisms of the HLA-B and HLA-DRB1 genes in Thai malaria patients. Jpn. J. Infect. Dis. *58*, 25–28.

Hawkins, B.R., Ma, J.T., Lam, K.S., Wang, C.C., and Yeung, R.T. (1985). Association of HLA antigens with thyrotoxic Graves' disease and periodic paralysis in Hong Kong Chinese. Clin. Endocrinol. (Oxf.) *23*, 245–252.

Henseler, T., and Christophers, E. (1995). Disease concomitance in psoriasis. J. Am. Acad. Dermatol. *32*, 982–986.

Hildebrand, W.H., Madrigal, J.A., Little, A.M., and Parham, P. (1992). HLA-Bw22: a family of molecules with identity to HLA-B7 in the alpha 1-helix. J. Immunol. *148*, 1155–1162.

Hilton, H.G., Vago, L., Older Aguilar, A.M., Moesta, A.K., Graef, T., Abi-Rached, L., Norman, P.J., Guethlein, L.A., Fleischhauer, K., and Parham, P. (2012). Mutation at positively selected positions in the binding site for HLA-C shows that KIR2DL1 is a more refined but less adaptable NK cell receptor than KIR2DL3. J. Immunol. *189*, 1418–1430.

Hilton, H.G., Guethlein, L.A., Goyos, A., Nemat-Gorgani, N., Bushnell, D.A., Norman, P.J., and Parham, P. (2015a). Polymorphic HLA-C Receptors Balance the Functional Characteristics of KIR Haplotypes. J. Immunol. *195*, 3160–3170.

Hilton, H.G., Norman, P.J., Nemat-Gorgani, N., Goyos, A., Hollenbach, J.A., Henn, B.M., Gignoux, C.R., Guethlein, L.A., and Parham, P. (2015b). Loss and Gain of Natural Killer Cell Receptor Function in an African Hunter-Gatherer Population. PLoS Genet. *11*, e1005439.

Hölzemer, A., Thobakgale, C.F., Jimenez Cruz, C.A., Garcia-Beltran, W.F., Carlson, J.M., van Teijlingen, N.H., Mann, J.K., Jaggernath, M., Kang, S., Körner, C., et al. (2015). Selection of an HLA-C*03:04-Restricted HIV-1 p24 Gag Sequence Variant Is Associated with Viral Escape from KIR2DL3+ Natural Killer Cells: Data from an Observational Cohort in South Africa. PLoS Med. *12*, e1001900.

Huang, X., Ling, H., Mao, W., Ding, X., Zhou, Q., Han, M., Wang, F., Cheng, L., and Xiong, H. (2009). Association of HLA-A, B, DRB1 alleles and haplotypes with HIV-1 infection in Chongqing, China. BMC Infect. Dis. *9*, 201.

Kaleab, B., Wondimu, A., Likassa, R., Woldehawariat, N., and Ivanyi, J. (1995). Sustained T-cell reactivity to Mycobacterium tuberculosis specific antigens in 'split-anergic' leprosy. Lepr. Rev. *66*, 19–25.

Karlsson, E.K., Kwiatkowski, D.P., and Sabeti, P.C. (2014). Natural selection and infectious disease in human populations. Nat. Rev. Genet. *15*, 379–393.

Koch, M., Camp, S., Collen, T., Avila, D., Salomonsen, J., Wallny, H.J., van Hateren, A., Hunt, L., Jacob, J.P., Johnston, F., et al. (2007). Structures of an MHC class I molecule from B21 chickens illustrate promiscuous peptide binding. Immunity *27*, 885–899.

Lin, M., Tseng, H.K., Trejaut, J.A., Lee, H.L., Loo, J.H., Chu, C.C., Chen, P.J., Su, Y.W., Lim, K.H., Tsai, Z.U., et al. (2003). Association of HLA class I with severe acute respiratory syndrome coronavirus infection. BMC Med. Genet. *4*, 9.

Lockless, S.W., and Ranganathan, R. (1999). Evolutionarily conserved pathways of energetic connectivity in protein families. Science *286*, 295–299.

Mathers, C., Fat, D.M., and Boerma, J.T. (2008). The global burden of disease: 2004 update (Geneva, Switzerland: World Health Organization).

Målen, H., Søfteland, T., and Wiker, H.G. (2008). Antigen analysis of Mycobacterium tuberculosis H37Rv culture filtrate proteins. Scand. J. Immunol. *67*, 245–252.

Malnati, M.S., Peruzzi, M., Parker, K.C., Biddison, W.E., Ciccone, E., Moretta, A., and Long, E.O. (1995). Peptide specificity in the recognition of MHC class I by natural killer cell clones. Science *267*, 1016–1018.

McCutcheon, J.A., Gumperz, J., Smith, K.D., Lutz, C.T., and Parham, P. (1995). Low HLA-C expression at cell surfaces correlates with increased turnover of heavy chain mRNA. J. Exp. Med. *181*, 2085–2095.

McMurtrey, C., Trolle, T., Sansom, T., Remesh, S.G., Kaever, T., Bardet, W., Jackson, K., McLeod, R., Sette, A., Nielsen, M., et al. (2016). Toxoplasma gondii peptide ligands open the gate of the HLA class I binding groove. eLife *5*, e12556.

Mendoza, J.L., Schmidt, A., Li, Q., Nuvaga, E., Barrett, T., Bridges, R.J., Feranchak, A.P., Brautigam, C.A., and Thomas, P.J. (2012). Requirements for efficient correction of ΔF508 CFTR revealed by analyses of evolved sequences. Cell *148*, 164–174.

Moesta, A.K., Norman, P.J., Yawata, M., Yawata, N., Gleimer, M., and Parham, P. (2008). Synergistic polymorphism at two positions distal to the ligand-binding site makes KIR2DL2 a stronger receptor for HLA-C than KIR2DL3. J. Immunol. *180*, 3969–3979.

Monot, M., Honoré, N., Garnier, T., Araoz, R., Coppée, J.Y., Lacroix, C., Sow, S., Spencer, J.S., Truman, R.W., Williams, D.L., and Gelber, R. (2005). On the origin of leprosy. Science *308* (5724), 1040–1042.

Naito, S., Sasaki, H., and Arakawa, K. (1987). Japanese Graves' disease: association with HLA-Bw46. Endocrinol. Jpn. *34*, 685–688.

Neisig, A., Melief, C.J., and Neefjes, J. (1998). Reduced cell surface expression of HLA-C molecules correlates with restricted peptide binding and stable TAP interaction. J. Immunol. *160*, 171–179.

Nielsen, M., Lundegaard, C., Worning, P., Lauemøller, S.L., Lamberth, K., Buus, S., Brunak, S., and Lund, O. (2003). Reliable prediction of T-cell epitopes using neural networks with novel sequence representations. Protein Sci. *12*, 1007–1017.

Nielsen, M., Lundegaard, C., Worning, P., Hvid, C.S., Lamberth, K., Buus, S., Brunak, S., and Lund, O. (2004). Improved prediction of MHC class I and class II epitopes using a novel Gibbs sampling approach. Bioinformatics *20*, 1388–1397.

Parham, P. (2005). MHC class I molecules and KIRs in human history, health and survival. Nat. Rev. Immunol. *5*, 201–214.

Parham, P., Adams, E.J., and Arnett, K.L. (1995). The origins of HLA-A,B,C polymorphism. Immunol. Rev. *143*, 141–180.

Rasmussen, M., Harndahl, M., Stryhn, A., Boucherma, R., Nielsen, L.L., Lemonnier, F.A., Nielsen, M., and Buus, S. (2014). Uncovering the peptide-binding specificities of HLA-C: a general strategy to determine the specificity of any MHC class I molecule. J. Immunol. *193*, 4790–4802.

Reibel, F., Cambau, E., and Aubry, A. (2015). Update on the epidemiology, diagnosis, and treatment of leprosy. Med. Mal. Infect. *45*, 383–393.

Ridley, D.S. (1974). Histological classification and the immunological spectrum of leprosy. Bull. World Health Organ. *51*, 451–465.

Scull, K.E., Dudek, N.L., Corbett, A.J., Ramarathinam, S.H., Gorasia, D.G., Williamson, N.A., and Purcell, A.W. (2012). Secreted HLA recapitulates the immunopeptidome and allows in-depth coverage of HLA A*02:01 ligands. Mol. Immunol. *51*, 136–142.

Shankarkumar, U. (2004). HLA associations in leprosy patients from Mumbai, India. Lepr. Rev. *75*, 79–85.

Shankarkumar, U., Ghosh, K., Badakere, S., and Mohanty, D. (2003). Novel HLA Class I Alleles Associated with Indian Leprosy Patients. J. Biomed. Biotechnol. *2003*, 208–211.

Sibilio, L., Martayan, A., Setini, A., Fraioli, R., Fruci, D., Shabanowitz, J., Hunt, D.F., and Giacomini, P. (2005). Impaired assembly results in the accumulation of multiple HLA-C heavy chain folding intermediates. J. Immunol. *175*, 6651–6658.

Sibilio, L., Martayan, A., Setini, A., Lo Monaco, E., Tremante, E., Butler, R.H., and Giacomini, P. (2008). A single bottleneck in HLA-C assembly. J. Biol. Chem. *283*, 1267–1274.

Sim, M.J., Malaker, S.A., Khan, A., Stowell, J.M., Shabanowitz, J., Peterson, M.E., Rajagopalan, S., Hunt, D.F., Altmann, D.M., Long, E.O., and Boyton, R.J. (2017). Canonical and Cross-reactive Binding of NK Cell Inhibitory Receptors to HLA-C Allotypes Is Dictated by Peptides Bound to HLA-C. Front. Immunol. *8*, 193.

Steiner, N.K., Baldassarre, L., Koester, R., Ng, J., Hartzman, R.J., and Hurley, C.K. (2002). Novel HLA-B alleles formed by an inter-locus recombination with HLA-C, HLA-B*0713 and B*6702. Tissue Antigens *59*, 148–150.

Takata, H., Sada, M., Ozawa, S., and Sekiguchi, S. (1978). HLA and mycobacterial infection: increased frequency of B8 in Japanese leprosy. Tissue Antigens *11*, 61–64.

Tregaskes, C.A., Harrison, M., Sowa, A.K., van Hateren, A., Hunt, L.G., Vainio, O., and Kaufman, J. (2016). Surface expression, peptide repertoire, and thermostability of chicken class I molecules correlate with peptide transporter specificity. Proc. Natl. Acad. Sci. USA *113*, 692–697.

Trolle, T., McMurtrey, C.P., Sidney, J., Bardet, W., Osborn, S.C., Kaever, T., Sette, A., Hildebrand, W.H., Nielsen, M., and Peters, B. (2016). The Length Distribution of Class I-Restricted T Cell Epitopes Is Determined by Both Peptide Supply and MHC Allele-Specific Binding Preference. J. Immunol. *196*, 1480–1487.

Trowsdale, J. (2011). The MHC, disease and selection. Immunol. Lett. *137*, 1–8.

Turner, S., Ellexson, M.E., Hickman, H.D., Sidebottom, D.A., Fernández-Viña, M., Confer, D.L., and Hildebrand, W.H. (1998). Sequence-based typing provides a new look at HLA-C diversity. J. Immunol. *161*, 1406–1413.

Venables, W., and Ripley, B. (2002). Modern Applied Statistics with S, Fourth Edition (New York: Springer).

Wahba, A., Dorfman, M., and Sheskin, J. (1980). Psoriasis and other common dermatoses in leprosy. Int. J. Dermatol. *19*, 93–95.

Wang, L.M., Kimura, A., Satoh, M., and Mineshita, S. (1999). HLA linked with leprosy in southern China: HLA-linked resistance alleles to leprosy. Int. J. Lepr. Other Mycobact. Dis. *67*, 403–408.

Wiker, H.G., Tomazella, G.G., and de Souza, G.A. (2011). A quantitative view on Mycobacterium leprae antigens by proteomics. J. Proteomics *74*, 1711–1719.

Yaciuk, J.C., Skaley, M., Bardet, W., Schafer, F., Mojsilovic, D., Cate, S., Stewart, C.J., McMurtrey, C., Jackson, K.W., Buchli, R., et al. (2014). Direct interrogation of viral peptides presented by the class I HLA of HIV-infected T cells. J. Virol. *88*, 12992–13004.

Zemmour, J., and Parham, P. (1992). Distinctive polymorphism at the HLA-C locus: implications for the expression of HLA-C. J. Exp. Med. *176*, 937–950.

Zemmour, J., Gumperz, J.E., Hildebrand, W.H., Ward, F.E., Marsh, S.G., Williams, R.C., and Parham, P. (1992). The molecular basis for reactivity of anti-Cw1 and anti-Cw3 alloantisera with HLA-B46 haplotypes. Tissue Antigens *39*, 249–257.

Zhang, F.R., Huang, W., Chen, S.M., Sun, L.D., Liu, H., Li, Y., Cui, Y., Yan, X.X., Yang, H.T., Yang, R.D., et al. (2009). Genomewide association study of leprosy. N. Engl. J. Med. *361*, 2609–2618.

Zinkernagel, R.M., and Doherty, P.C. (1974). Restriction of in vitro T cell-mediated cytotoxicity in lymphocytic choriomeningitis within a syngeneic or semiallogeneic system. Nature *248*, 701–702.